香港氣象學會

The Hong Kong Meteorological Society

Bulletin

VOLUME 24, ISSN 1024-4468

ISSN 1024-4468

The Hong Kong Meteorological Society Bulletin is the official organ of the Society, devoted to articles, editorials, news and views, activities and announcements of the Society.

Members are encouraged to send any articles, media items or information for publication in the Bulletin. For guidance see the information for contributors in the inside back cover.

Advertisements for products and/or services of interest to members of the Society are accepted for publication in the Bulletin.

For information on formats and rates please contact the Society secretary at the address opposite.

Views and opinions expressed in the articles or any correspondence are those of the author(s) alone and do not necessarily represent the views and opinions of the Society.

The mention of specific products and/or companies does not imply there is any endorsement by the Society or its office bearers in preference to others which are not so mentioned.

SUBSCRIPTION RATES

Institutional rate:	HK$ 300 per volume
Individual rate:	HK$ 150 per volume

Published by

The Hong Kong Meteorological Society
c/o Hong Kong Observatory
134A Nathan Road
Kowloon, Hong Kong

Homepage
http://www.meteorology.org.hk

香港氣象學會

The Hong Kong Meteorological Society

Bulletin

VOLUME 24, 2014

Contents

Editorial

The first paper by H.S. Chan, H.W. Tong, and S.M. Lee of the Hong Kong Observatory presents the temperature projection for Hong Kong in the 21st century using CMIP5 models, following the release of The Fifth Assessment Report of the Intergovernmental Panel on Climate Change Working Group I in September 2013.

The second paper by Marco Leung and Wen Zhou of the City University of Hong Kong investigates the variations of East Asian winter monsoon and midlatitude atmospheric circulation concurrent with different latitudinal position of the East Asian trough.

The third paper by Edwin Lai, T.C. Lee and Y.H. Lau of the Hong Kong Observatory reviews the characteristics of the wind climate of Hong Kong using the automatic weather station data, and analyse wind trends over different parts of Hong Kong.

The Hong Kong Meteorological Society co-organized with the Hong Kong Science Museum to give a Popular Science Lecture Series with the theme 'Decoding Natural Disasters – Piecing Together the Climate Change Jigsaw Puzzle' on 15 November 2014. Three professionals were invited to deliver the talks. A tour to the Jockey Club Museum of Climate Change at the Chinese University was organized on 22 November 2014. Some photos of the talks and the visit are included in this issue.

A painting competition for primary students with the topic ' 齊抗天災 ' was organized in collaboration with the Hong Kong Society for Education in Art. There were over 70 entries for the competition. The awards presentation ceremony was held on 7 September 2014. The colour pages in the end of this issue show the winning entries of the competition.

About the cover

The cover is a photograph of a cumulonimbus taken at the Airport Meteorological Office by Mr. Chiang Kwok-fai on 27 May 2014.

Temperature projection for Hong Kong in the 21st century using CMIP5 models

CHAN Ho-sun, TONG Hang-wai, LEE Sai-ming
Hong Kong Observatory

ABSTRACT

The Fifth Assessment Report (AR5) of the Intergovernmental Panel on Climate Change (IPCC) Working Group I (WGI) was released in September 2013. Its assessment was based on a new set of global climate simulations from the Coupled Model Intercomparison Project Phase 5 (CMIP5) as well as a new set of greenhouse gas (GHG) concentration scenarios named Representative Concentration Pathways (RCPs). Projections of Hong Kong's climate need to be updated and evaluated based on the new scenarios and the corresponding new model simulations.

This study focuses on the temperature projection for Hong Kong. The annual mean temperatures in Hong Kong in the 21st century under the RCP4.5 and RCP8.5 scenarios are derived through statistical downscaling on a monthly basis. Projection results suggest that the annual mean temperature will continue to rise for the rest of the 21st century. The central 90% of the projected temperature increase by 2100 based on the RCP4.5 scenario will be 1.4 to 3.2 °C, relative to the average temperature of 1986-2005. For the RCP8.5 scenario, which matches the current situation most closely in terms of carbon dioxide ($CO_{2)}$ emission, the central 90% of the projected temperature increase by 2100 will be 3.1 to 5.5 °C. These results are comparable with those of previous studies of temperature projections for southern China using direct model outputs of the CMIP5 dataset. The new projection results will be compared with those from the Coupled Model Intercomparison Project Phase 3 (CMIP3) and discussed.

KEY WORDS : Hong Kong · temperature projection · statistical downscaling · CMIP5

Email: hwtong@hko.gov.hk

1. Introduction

The IPCC WGI AR5 (IPCC 2013) reaffirms that there is unequivocal global warming and concludes that it is extremely likely that human influence has been the dominant cause of the observed warming since the mid-20th century. Regarding the projection of future climate, AR5 relies on a new set of global climate models participating in CMIP5. In addition, a new set of four GHG concentration scenarios is designed to fulfill the growing interest in scenarios that explicitly explore the impact of different climate policies (Moss *et al.*, 2010) and to provide higher-resolution and more consistent land-use and land-cover data to ever improving and more comprehensive climate models (Van Vuuren *et al.* 2011). Based on the new set of models and the new set of GHG concentration scenarios, AR5 projects that the global average surface temperature will rise by 0.3 – 4.8 °C towards the end of this century (IPCC 2013).

Almost the whole globe experienced warming in the last hundred years or so, and Hong Kong is no exception. The annual mean temperature of Hong Kong has increased at a rate of 0.12 °C per decade over the years 1885-2012. Along with the increase in annual mean temperature, extremely hot days have become more frequent while extremely cold days have become rarer (Lee *et al.*, 2011b). Elevated temperatures have implications for public health because of the anticipated increase in heat-related diseases, and for energy consumption because of the increasing need for cooling. Temperature projection is therefore an important piece of information to support planning for adaptation to climate change (World Bank 2012; IPCC 2012).

In 2004, the Hong Kong Observatory utilized the data of global climate model projections assessed by the IPCC's Third Assessment Report to project the temperature for Hong Kong in the 21st century (Leung *et al.*, 2004). The projection was subsequently updated using monthly model data from IPCC's Fourth Assessment Report (AR4) in 2007 with urbanization effects incorporated (Leung *et al.*, 2007). AR4 daily data were later used to project extreme temperature events for Hong Kong (Lee *et al.*, 2011a). In the last study, the projection of annual mean temperature using a different methodology and urbanization scenario was investigated and compared to the previous results. In light of the new set of climate models and GHG concentration scenarios, another update of the temperature projection for Hong Kong is needed.

Statistical downscaling, which relates large-scale dynamical model parameters to station-specific variables of interest, is a cost-effective approach to studying climate projection. It requires many fewer computer resources than dynamical downscaling while achieving a comparable level of skill (Murphy 1999). In line with previous climate projection studies for Hong Kong, statistical downscaling is also adopted in the present study.

This paper is organized as follows: data used in this study will be described in Section 2, followed by an evaluation of the CMIP5 models in temperature simulation in Section 3; the projection method will be presented in Section 4; the projection results will be compared with other AR5 climate projection studies and previous temperature projections for Hong Kong in Section 5; and a summary will be given in Section 6.

2. Data

2.1 Predictand and predictors

The monthly mean temperature of Hong Kong is the predictand of the statistical downscaling model in this study. Historical temperature data recorded at the Hong Kong Observatory Headquarters during the period 1961-2005 are partitioned appropriately into two groups (1961-1990 and 1991-2005) to support construction and validation of the statistical model. Surface and upper-air parameters of reanalysis data or General Circulation Models (GCMs) averaged over

southern China and the northern part of the South China Sea (108-120°E, 16-30°N) are the large-scale predictors of the statistical model.

2.2 Reanalysis data

The NCEP 20th Century Reanalysis (20CR) Data (Compo *et al.*, 2011) are employed in (i) verifying CMIP5 models' performance in temperature simulation; and (ii) constructing the statistical downscaling model of the monthly temperature in Hong Kong. The NCEP 20CR data have a horizontal resolution of 2 degrees x 2 degrees.

2.3 CMIP5 model data

As of the start of the study (September 2013), 25 CMIP5 models, in which all the potential predictor sets were included, were available for download. Monthly data from these 25 CMIP5 models with different horizontal resolutions (Table 1) from the Program for Climate Model Diagnosis and Intercomparison website (http://pcmdi9.llnl.gov) were acquired and then regridded using bilinear interpolation to 2 degrees x 2 degrees in order to match the horizontal resolution of the NCEP 20CR data. Historical simulations of the CMIP5 models during the period 1961-2005 are used to validate the statistical downscaling model while future simulations under different GHG emission scenarios are used to produce future temperatures for Hong Kong.

In AR5, there are four GHG concentration scenarios, namely RCP2.6, RCP4.5, RCP6.0, and RCP8.5, which are identified by their approximate total radiative forcing in the year 2100 relative to the year 1750: 2.6 Wm^{-2} for RCP2.6, 4.5 Wm^{-2} for RCP4.5, 6.0 Wm^{-2} for RCP6.0, and 8.5 Wm^{-2} for RCP8.5 (IPCC 2013; Moss *et al.*, 2010; Van Vuuren *et al.*, 2011). The RCP4.5 and RCP8.5 scenarios belong to the core experiments of CMIP5 for which all the participating modelling groups should provide model simulations (Taylor *et al.*, 2008) and therefore have the largest number of model simulations for assessment of future climate (25 models in this study). RCP 2.6 and RCP 6.0 have fewer modelling groups to take part, with only 17 models available at the beginning of the study. It is noteworthy that the current path of global CO_2 emission most closely matches the CO_2 emission trajectory described by the RCP8.5 scenario (Peters *et al.*, 2012). In this study, only the projection results of RCP4.5 and RCP8.5 will be discussed. Nonetheless, projection results of RCP2.6 and RCP6.0 will be included in the Appendix for reference.

3. Evaluation of CMIP5 models' performance in temperature simulation

It is imperative that large-scale predictors of the statistical model are reasonably simulated by the climate models as they are used to condition the local predictand. Naturally, surface temperature is the most important predictor, as it is directly related to the variable to be projected. As shown in Fig. 1, the annual cycle of temperature over southern China (land grid points over 108-120°E, 16-30°N) during the period 1961-1990 is reasonably simulated by the 25 CMIP5 models. However, a cold bias in winter months can be seen in almost all models when compared to the NCEP 20CR data. In Fig. 2, a Taylor diagram indicates that the performance of the CMIP5 models is satisfactory in terms of spatial correlation. All 25 models achieve a spatial correlation of over 0.9. In addition, the performance of the models is rather homogeneous, without any obvious outliers depicted in Fig. 2.

Ideally, other potential predictors such as specific humidity, geopotential height, and winds at various levels should also be evaluated before statistical downscaling (Wilby *et al.*, 2004). But detailed evaluation of every potential predictor is far beyond the scope of the current study. Nevertheless, many studies have shown that the CMIP5 models continued to improve after the Fourth Assessment Report of IPCC (Kug *et al.*, 2012; Sperber *et al.*, 2012). Here, without detailed investigation, we trust that

CMIP5 models can reasonably reproduce large-scale climatological features.

4. Methodology

Hong Kong is a developed city, and the urbanization effect on its temperature cannot be ignored, although previous studies have shown that global warming has had a bigger contribution to the city's rising temperature trend over the years. Global climate models usually do not take the urbanization effect into account. Hence, in projecting the temperature for Hong Kong, the urbanization effect on temperature and the statistical downscaling process have to be dealt with separately. The basic idea is to remove the urbanization effect in the historical temperature records before carrying out the statistical downscaling procedures, and then incorporate the future urbanization effect in the result of the downscaling process. Key steps and considerations in dealing with the urbanization effect and the statistical downscaling procedures are described in the following subsections. Fig. 3 illustrates the workflow in a schematic diagram.

4.1 Urbanization effect in the past and future

The urbanization effect on Hong Kong's historical temperature trend is estimated using Macao as the rural station (Lee *et al.* 2011a). Macao is located about 65 km west of Hong Kong and was relatively less affected by urbanization before 2000 (Fong *et al.*, 2009). Temperature data from Macao during the period 1952-2000 are used to estimate the background rising temperature trend due to global warming, and the difference between Hong Kong's temperature trend and Macao's is considered to be the contribution from urbanization (Lee *et al.*, 2011a).

Some studies have suggested (Oke 1973; Torok *et al.*, 2001) that the urbanization effect is directly proportional to the logarithm of population (log P). Hence, the rate of temperature rise due to urbanization can be related to the rate of change in log P. The future population of Hong Kong up until 2041 is projected by the Census and Statistics Department of Hong Kong, and the population projection data are available for download on its website (http://www.censtatd.gov.hk/hkstat/sub/sp190.jsp). It can be estimated from Fig. 4 that the average rate of increase in log P between 2001 and 2041 is about 30% of the rate during 1952-2000.

Since there is no population projection for years after 2041, two urbanization scenarios are considered: (1) urbanization continues at the same rate as that between 2001 and 2041 for years beyond 2041 (U1), and (2) urbanization stops after 2041 (U2).

4.2 Predictor selection for the downscaling model

To investigate the sensitivity of downscaling results to the choice of predictors, a number of combinations of thermodynamical parameters and low-level circulation parameters that also carry the climate change signal, though probably to a weaker extent (Gutierrez *et al.*, 2013; Wilby *et al.*, 1998; Wilby *et al.*, 2004), are considered. Three predictor sets are examined:

- Set 1: Surface temperature
- Set 2: Surface temperature, mean sea level pressure
- Set 3: Surface temperature, mean sea level pressure, surface specific humidity, 850 hPa wind (zonal and meridional), 850 hPa specific humidity, 850 hPa geopotential height

The first predictor set consists of surface temperature only, which is a natural choice of predictor when projecting future temperature changes. The second set consists of surface temperature and mean sea level pressure. Here mean sea level pressure serves as a circulation variable.

Inclusion of a circulation variable, as suggested by some studies, may lead to improvement of the downscaling results (Huth 1999). The third set is the most complex. Besides surface temperature and mean sea level pressure, it also includes 850 hPa zonal wind, meridional wind, geopotential height, and specific humidity. These predictors are common in statistical downscaling studies (Gutierrez *et al.*, 2013; Huth 2002).

The three predictor sets are increasingly complex while maintaining a balance between the number of thermodynamical and circulation parameters participating in the regression model. Gutierrez *et al.* (2013) suggested that 2-metre air temperature is a preferable predictor to free-tropospheric temperatures like temperature at 850 hPa. Hence, upper-air temperature is not included in the predictor sets so as to keep the sets from becoming too large.

4.3 Regression

The NCEP 20CR data are free from the urbanization effect because air temperature observations were not involved in the data assimilation process (Compo *et al.*, 2011; Compo *et al.*, 2013) and hence are a good candidate for building a regression model with the deurbanized temperature data. The monthly data are aggregated into four seasons (MAM, JJA, SON, and DJF) to establish four regression models, each valid for the months constituting that season.

4.3.1 Standardization

In order to reduce systematic bias, it is common practice to standardize the predictors and predictand in building and applying a regression model. In this study, the deurbanized Hong Kong temperature data, the NCEP 20CR data, and the CMIP5 model parameters are standardized with reference to the period 1961-1990. Outcomes from the regression model will need to be destandardized.

4.3.2 Variance adjustment

Normally, the variance of regression outcomes is smaller than the observations (Huth 2002; Easterling 1999), and variance adjustment is performed to preserve the variance. In the present study, we have adopted the variance inflation method in which the regression outcomes will be multiplied by the factor

$$\frac{\text{standard deviation of observations}}{\text{standard deviation of regression outcomes}}$$

where the standard deviations are computed over a common reference period (1961-1990 in this study).

In a temperature projection study, extra care has to be taken to preserve the long-term trend of the regression outcomes (Easterling 1999). The following procedures are conducted in this study:

- the regression outcomes are first detrended using simple linear regression;
- variance inflation is applied to the detrended outcomes resulting from (a);
- the linear trend obtained in (a) is then added back to the inflated outcomes resulting from (b).

5. Results

5.1. Validation of the statistical model

The historical run of each of the 25 CMIP5 models is downscaled using the Set 1 predictor for the period 1961-2005. The ensemble mean of the downscaling results of the 25 CMIP5 models, also with the urbanization effect incorporated, is considered. Fig. 5 shows the 5-year average of the ensemble mean (the green line). It is clear that the actual warming trend during the period 1991-2005 can be reproduced nicely. Fig. 6 shows the annual cycle of the ensemble mean during the period 1991-2005. The actual annual cycle is reasonably reproduced except for some minor deviations in winter months. The root-mean-square error (RMSE) during this validation period for predictor set

1, set 2, and set 3 is 0.31°C, 0.31°C, and 0.30°C, respectively (Table 2). There is zero bias for all three predictor sets (Table 2). The differences between the downscaled temperature using different predictor sets are minimal (not shown), suggesting that the downscaled temperatures are insensitive to the choice of predictor set.

5.2. Projection for the 21st century

Table 3a (3b) shows the temperature changes in Hong Kong in the near term (2021-2030), the mid-21st century (2051-2060), and the end of the 21st century (2091-2100), given by the ensemble mean of projections of the 25 CMIP5 models under the RCP4.5 (RCP8.5) scenario and the U1 urbanization scenario using different predictor sets. The changes are relative to the average temperature of 1986-2005. Following the convention adopted by IPCC WGI AR5, the 5th and 95th percentiles of the ensemble are used to indicate the likely range of projection. Very little difference exists among the results from the three predictor sets, showing that the projection is not sensitive to the choice of predictors.

Table 4 shows the temperature changes in Hong Kong in 2091-2100 given by the ensemble mean of projections of the 25 CMIP5 models under RCP4.5 and RCP8.5 scenarios and urbanization scenarios using different predictor sets. The difference between the results from the two urbanization scenarios is also small, just 0.1 °C in the ensemble mean. This indicates that urbanization plays a very limited role in future warming when compared to GHG under RCP4.5 and RCP8.5 scenarios. Under the RCP4.5 (RCP8.5) scenario and the U1 urbanization scenario, urbanization contributes around 10% (5%) to the total warming during 2006-2100.

We pooled all the results from different predictor sets under the U1 urbanization scenario to form the temperature projection for Hong Kong. Fig. 7 (8) shows the projected temperature change in Hong Kong for the 21st century under the RCP4.5 (RCP8.5) scenario. For the RCP4.5 (RCP8.5) scenario, the ensemble mean of temperature rise could reach 2.2 °C (4.2 °C) in 2091-2100, with a likely range of 1.4 - 3.2 °C (3.1 - 5.5 °C).

5.3. Comparison with other studies

Some studies have projected temperature changes for East Asia or China by considering the direct model output of CMIP5 models or results from dynamical downscaling using regional climate models. For instance, IPCC WGI AR5 provided regional temperature projections for East Asia in its atlas of global and regional climate projections. Xu and Xu (2012) focused on China and investigated the direct model output of 11 CMIP5 models and their temperature and precipitation projections in the 21st century. Gao *et al.* (2013) utilized a regional climate model (RegCM4.0) driven by a global model, Beijing Center Climate System Model version 1.1 (BCC_CSM1.1, M2 in Table 1), to downscale the temperature projection for China in the 21st century under the RCP4.5 and RCP8.5 scenarios.

A comparison of the present study with other studies of temperature projection over southern China (IPCC 2013; Xu and Xu 2012; Gao *et al.* 2013) is shown in Table 5. The temperature projections of these studies for the vicinity of Hong Kong are read from spatial maps of temperature projection. The reference period of all the studies is the same, 1986-2005. The temperature projections in this study are comparable to those in IPCC (2013) and Gao *et al.* (2013), but higher than those in Xu and Xu (2012). It should be noted that the projections given by Gao *et al.* (2013) are the result of a single regional climate model driven by a single global climate model, which makes it difficult to assess the uncertainty of the projections. Furthermore, there exists a cold bias of around 1-2.5 °C along the coastal region of Guangdong in the regional climate model as revealed by the validation, and this may be a systematic bias that affects the

subsequent temperature projections (see Fig. 1c of Gao *et al.* (2013)).

5.4. Comparison with previous projections using AR4 data

It is of interest to compare the results of this study with previous temperature projections computed using AR4 data, i.e., Leung *et al.* (2007) and Lee *et al.* (2011a). To facilitate direct comparison, the reference period used in the present study was shifted from 1986-2005 to 1980-1999 in order to match previous studies. Table 6 lists the temperature projection results at the end of the 21st century given by these three studies.

The RCP4.5 (RCP8.5) scenario in AR5 resembles the B1 (A2) scenario in AR4 in terms of CO_2 emission. However, the CO_2 emission trajectory of RCP4.5 (RCP8.5) is lower (higher) than that of B1 (A2) for a large portion of the 21st century. Hence, it should not be surprising that the temperature projection under the RCP4.5 (RCP8.5) scenario is lower (higher) than the projection under the B1 (A2) scenario in Lee *et al.* (2011a). However, projections in Leung *et al.* (2007) are significantly higher than the projections in this study. The disparity could be attributed to the difference in the assumption of future urbanization. In Leung *et al.* (2007), future urbanization in Hong Kong was assumed to be the same as what was experienced in the past. This assumption may not hold, as shown in Fig. 4. It is more reasonable to argue that urbanization will gradually saturate at some point in the future.

6. Summary

In this study, 25 CMIP5 models are statistically downscaled to Hong Kong to project the temperature change in the 21st century. The effect of urbanization has been duly considered and incorporated. Results show that the temperature increase in 2091-2100 is likely in the range of 1.4 - 3.2 °C (3.1 - 5.5 °C) under the RCP4.5 (RCP8.5) scenario. Owing to the projected slow-down of population growth, the contribution of urbanization to the total warming will be less than that in the past century. It is estimated that urbanization will contribute only around 5% (10%) to the total warming under the RCP8.5 (RCP4.5) scenario.

The projection results in this study are comparable to those of some AR5 studies using direct model outputs, boosting the confidence in our projections. Temperature projections from previous studies have also been reviewed and the differences accounted for.

Numerous studies have shown that the shift in mean temperature distribution will inevitably change the probability of extreme temperature events (IPCC 2012; Hansen *et al.* 2012). Previous studies have shown that Hong Kong is expected to have more extremely hot events and fewer extremely cold events using AR4 daily data (Lee *et al.* 2011a). Work is underway to update the projection of extreme temperature events using AR5 daily data.

Acknowledgments: The authors would like to thank CM Shun, Edwin ST Lai, and TC Lee of the Hong Kong Observatory for providing comments. We acknowledge the World Climate Research Programme's Working Group on Coupled Modelling, which is responsible for CMIP, and we thank the climate modeling groups (listed in Table 1 of this paper) for producing and making available their model output.

References

Compo, G. P. and Coauthors, 2011: The twentieth century reanalysis project. *Q. J. R. Meteorol. Soc.*, **137,** 1-28

Compo, G. P., P. D. Sardeshmukh, J. S. Whitaker, P. Brohan, P. D. Jones and C. Mccoll, 2013: Independent confirmation of global land warming without the use of station temperatures. *Geo. Res. Lett.*, **40**, 3170-3174

Easterling. D, 1999: Development of regional climate scenarios using a downscaling approach. *Clim. Change*, **41**, 615-634

Fong, S. K., C. H. Wu, A. Wang, Z. H. He, T. Wang, K .C. Leong and U. M. Lai, 2009: Analysis of surface air temperature change in Macau during 1901-2007. Advance in *Climate Change Research,* **5(1)** 12-17

Gao X. J., M. L. Wang and F. Giorgi, 2013: Climate change over China in the 21st century as simulated by BCC_CSM1.1-RegCM4.0. *Atmos. Oceanic Sci. Lett.*, **6**, 381-386

Gutierrez, J. M., D. S. Martin, S. Brands, R. Manzanas and S. Herrera, 2013: Reassessing statistical downscaling techniques for their robust application under climate change conditions. *J. Clim.*, **26,** 171-188

Hansen, J., M. Sato and R. Ruedy, 2012: Perception of climate change. *Proc. Natl. Acad. Sci.*, **109**, 14726-14727

Huth. R., 1999: Statistical downscaling in central Europe: Evaluation of method and potential predictors. *Clim. Res.*, **13,** 91-101

Huth. R., 2002: Statistical downscaling of daily temperature in central Europe. *J. Clim.*, **15,** 1731-1742

IPCC, 2012: *Special report on managing the risks of extreme events and disasters to advance climate change adaptation (SREX)*

IPCC, 2013: *Summary for Policymakers. In: Climate Change 2013: The physical basis. Contribution of Working Group I to the Fifth Assessment Report of the Intergovernmental Panel on Climate Change*. Cambridge University Press, Cambridge, United Kingdom and New York, NY, USA.

Kug, J. S., Y. G. Ham, J. Y. Lee and F. F. Jin, 2012: Improved simulation of two types of El Niño in CMIP5 models. *Environ. Res. Lett.*, 7, 1-7

Lee, T. C., K. Y. Chan and W. L. Ginn, 2011a: Projection of extreme temperature in Hong Kong in the 21st century. *Acta Meteorologica Sinica* **25(1)** 1-20

Lee, T.C., H. S. Chan, E. W. L. Ginn and M. C. Wong, 2011b: Long-term trends in extreme temperatures in Hong Kong and southern China. *Adv. Atmos. Sci.*, **28(1),** 147-157

Leung, Y. K., E. W. L. Ginn, M. C. Wu, K. H. Yeung and W. L. Chang, 2004: Temperature projections for Hong Kong in the 21st century. *Bull. HK. Met. Soc.*, **14**, 21-48

Leung, Y. K., M. C. Wu, K. K. Yeung and W. M. Leung, 2007: Temperature projections for Hong Kong based on IPCC Fourth Assessment Report. Bull. HK. *Met. Soc.*, **17**, 13-22.

Moss, R. H. and Coauthors, 2010: The next generation of scenarios for climate change research and assessment. *Nature*, **465**, 747-756

Murphy, J. M., 1999: An evaluation of statistical and dynamical techniques for downscaling local climate. J. Clim., **12**, 2256-2284

Oke, T. R., 1973: City size and the urban heat island. *Atmos. Environ.*, **7**, 769-779

Peters, G. P., R. M. Andrew, T. Boden, J. G. Canadell, P. Ciais, C. Le Quere, G. Marland, M. R. Raupach and C. Wilson, 2012: The challenge to keep global warming below 2 °C. Nat. *Clim. Change*, **3**, 4-6

Sperber, K. R., H. Annamalai, L. S. Kang, A. Kitoh, A. Moise, A. Turner, B. Wang and T. Zhou, 2012: The Asian summer monsoon: An intercomparison of CMIP5 vs. CMIP3 simulations of the late 20th century. *Clim. Dyn.*, **41**, 2711-2744

Taylor, K. E., R. J. Stouffer and G. A. Meehl, 2008: A summary of the CMIP5 experiment design. Available at: http://cmip-pcmdi.llnl.gov/cmip5/docs/Taylor_CMIP5_dec31.pdf

Torok, S. J., C. J. Morris, C. Skinner and N. Plumber, 2001: Urban heat island features of Southeast Australian towns. *Aust. Met. Mag.*, **50**, 1-13

Van Vuuren, D. P. and Coauthors, 2011: The representative concentration pathways: An overview. *Clim. Change*, **109**, 5-31

Wilby, R. L., S. P. Charles, E. Zorita, B. Timbal, P. Whetton, L. O. Mearns, 2004: Guidelines Use of Climate Scenarios Developed from Statistical Downscaling Methods.

Available at: http://www.narccap.ucar.edu/doc/tgica-guidance-2004.pdf

Wilby, R. L., T. M. L. Wigley, D. Conway, P. D. Jones, B. C. Hewitson, J. Main and D. S. Wilks, 1998: Statistical downscaling of general circulation model output: A comparison of methods. *Wat. Res.*, **34(11)**, 2995-3008

World Bank, 2012: Turn down the heat: Why a 4°C warmer world must be avoided. Washington DC. https://openknowledge.worldbank.org/handle/10986/11860

Xu, Y. and C. H. Xu, 2012: Preliminary assessment of simulation of climate changes over China by CMIP5 multi-models. Atmos. Oceanic Sci. Lett., 5, 489-494

Table 1. Details of the 25 CMIP5 models used in this study for RCP4.5 and RCP8.5

				Resolution	
	Model	Center	Country	Latitude	Longitude
M1	ACCESS1-0	CSIRO	Australia	1.25	1.875
M2	BCC-CSM1-1	BCC	China	~ 2.8	2.8125
M3	BNU-ESM	BNU	China	~ 2.8	2.8125
M4	CanESM2	CCCma	Canada	~ 2.8	2.8125
M5	CCSM4	NCAR	USA	~0.94	1.25
M6	CNRM-CM5	CNRM	France	~1.4	1.40625
M7	CSIRO-Mk36	CSIRO	Australia	~1.86	1.875
M8	FGOALS_g2	IAP	China	~ 2.8	2.8125
M9	GFDL-ESM2G	NOAA GFDL	USA	~2	2.5
M10	GFDL-ESM2M	NOAA GFDL	USA	~2	2.5
M11	GISS-E2-H	NASA GISS	USA	2	2.5
M12	GISS-E2-R	NASA GISS	USA	2	2.5
M13	HadGEM2-AO	NIMR KMA	South Korea	1.25	1.875
M14	HadGEM2-CC	UKMO Had	UK	1.25	1.875
M15	HadGEM2-ES	UKMO Had	UK	1.25	1.875
M16	INM-CM4	INM	Russia	1.5	2
M17	IPSL-CM5A-LR	IPSL	France	~1.88	3.75
M18	IPSL-CM5A-MR	IPSL	France	~1.27	2.5
M19	IPSL-CM5B-LR	IPSL	France	~1.88	3.75
M20	MIROC5	MIROC	Japan	~1.4	1.40625
M21	MIROC-ESM	MIROC	Japan	~ 2.8	2.8125
M22	MIROC-ESM-CHEM	MIROC	Japan	~ 2.8	2.8125
M23	MRI-CGCM	MRI	Japan	~1.12	1.125
M24	Nor-ESM1-M	NCC	Norway	~1.88	2.5
M25	Nor-ESM1-ME	NCC	Norway	~1.88	2.5

Table 2. Root-mean-square error (RMSE) and mean bias of downscaled temperature using different predictor sets during the validation period 1991-2005.

	Set 1	Set 2	Set 3
RMSE (°C)	0.31	0.31	0.30
Bias (°C)	0.0	0.0	0.0

Table 3a Temperature changes (°C) in Hong Kong in the near term (2021-2030), the mid-21st century (2051-2060), and the end of the 21st century (2091-2100), given by the ensemble mean of projections of the 25 CMIP5 models under the RCP4.5 scenario and the U1 urbanization scenario using different predictor sets. Changes are relative to the average temperature of 1986-2005. Figures in parentheses indicate the likely range (the 5th and 95th percentiles of the ensemble).

	2021-2030	2051-2060	2091-2100
Set 1	0.8 (0.5-1.2)	1.7 (1.0-2.3)	2.2 (1.4-3.0)
Set 2	0.8 (0.5-1.2)	1.7 (1.0-2.3)	2.2 (1.4-3.0)
Set 3	0.8 (0.5-1.2)	1.6 (1.1-2.3)	2.2 (1.3-3.2)

Table 3b. Same as Table 3a but for the RCP8.5 scenario.

	2021-2030	2051-2060	2091-2100
Set 1	0.9 (0.5-1.3)	2.2 (1.6-3.0)	4.2 (3.1-5.5)
Set 2	0.9 (0.5-1.3)	2.2 (1.6-3.0)	4.2 (3.1-5.5)
Set 3	0.9 (0.6-1.3)	2.2 (1.6-3.1)	4.2 (3.1-5.6)

Table 4. Temperature changes (°C) in Hong Kong in 2091-2100 given by the ensemble mean of projections of the 25 CMIP5 models under RCP 4.5 and RCP 8.5 scenarios and urbanization scenarios using different predictor sets. Changes are relative to the average temperature of 1986-2005. Figures in parentheses indicate the likely range (the 5th and 95th percentiles).

	Set 1		Set 2		Set 3	
	U1	U2	U1	U2	U1	U2
RCP4.5	2.2 (1.4-3.0)	2.1 (1.3-2.9)	2.2 (1.4-3.0)	2.1 (1.3-2.9)	2.2 (1.3-3.2)	2.1 (1.2-3.1)
RCP8.5	4.2 (3.1-5.5)	4.1 (3.0-5.3)	4.2 (3.1-5.5)	4.1 (2.9-5.4)	4.2 (3.1-5.6)	4.1 (3.0-5.5)

Table 5. Projected temperature change (°C, relative to the average of 1986-2005) for the end of the 21st century by other studies.

	IPCC (2013)		Xu and Xu (2012)		Gao et al. (2013)	
Period	2081-2100		2071-2100		2081-2099	
Scenario	RCP4.5	RCP8.5	RCP4.5	RCP8.5	RCP4.5	*RCP8.5*
Projection	1.5-2.0	3.0-4.0	2.0-2.4	3.6-4.0	<1.5	*2.5-3.0*

Table 6. Comparison of the ensemble mean of temperature projections (°C, relative to the average of 1980-1999) given by the present study and previous studies using AR4 data.

	Present study		Leung (2007)		Lee (2011a)	
Period	2091-2100		2090-2099		2090-2099	
Scenario	RCP4.5	RCP8.5	B1	A2	B1	A2
Projection	2.3	4.4	3.0	5.2	2.5	4.2

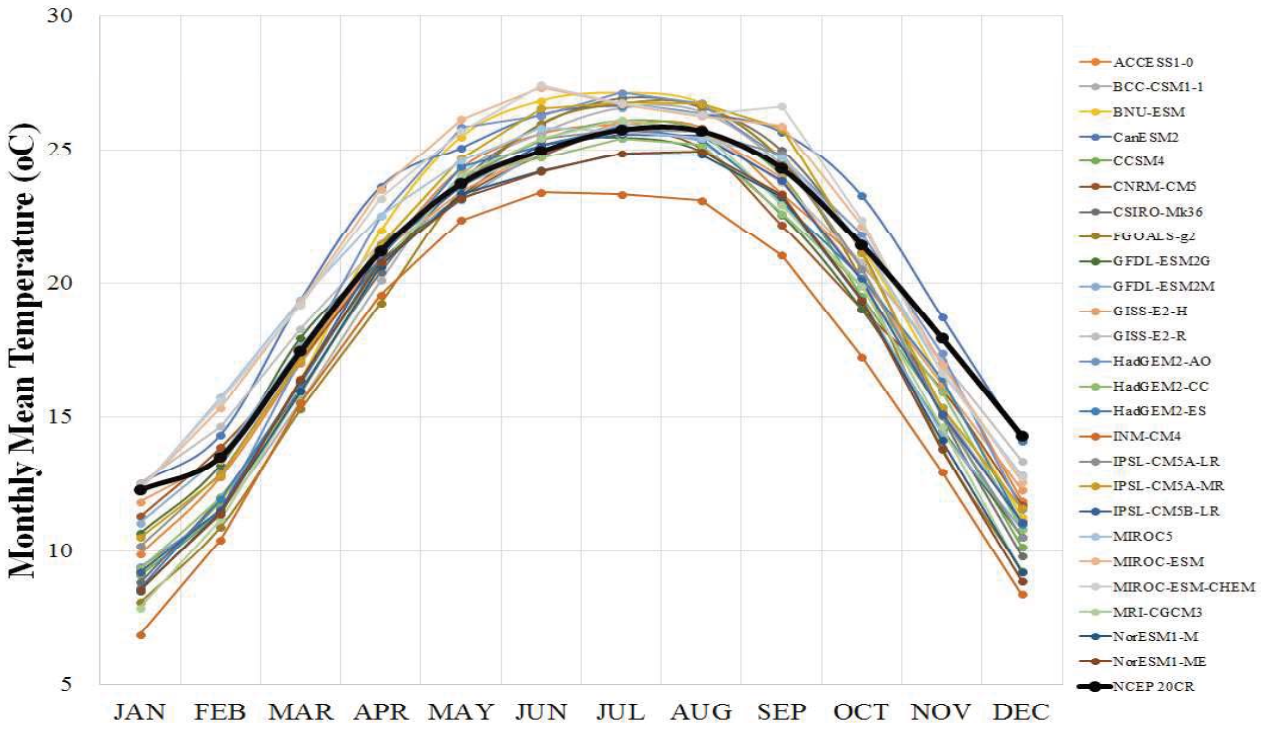

Fig. 1. Annual cycle of monthly temperature over southern China during 1961-1990 simulated by the 25 CMIP5 models. The thick black line is NCEP 20th Century Reanalysis.

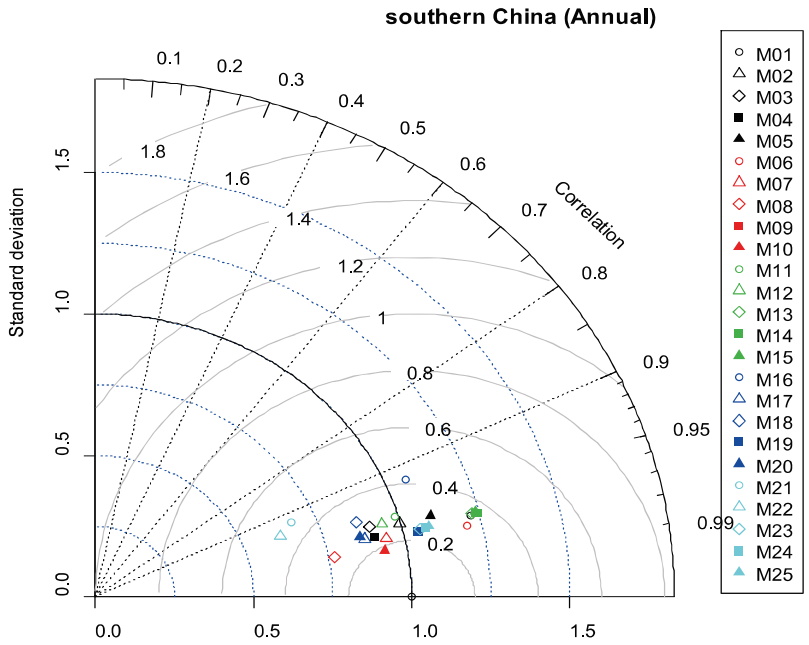

Fig. 2. *Taylor diagram showing performance of the 25 CMIP5 models in simulating annual mean temperature over southern China during 1961-1990. Names of the models can be found in Table 1.*

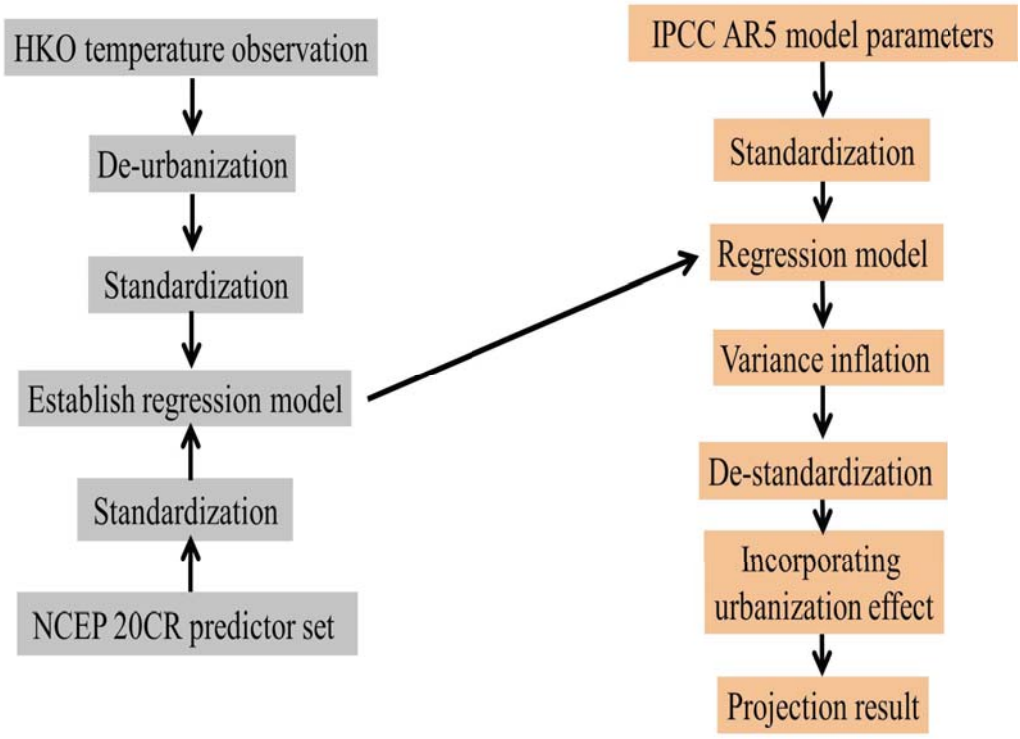

Fig. 3. *Schematic diagram showing the workflow of projecting temperature for Hong Kong*

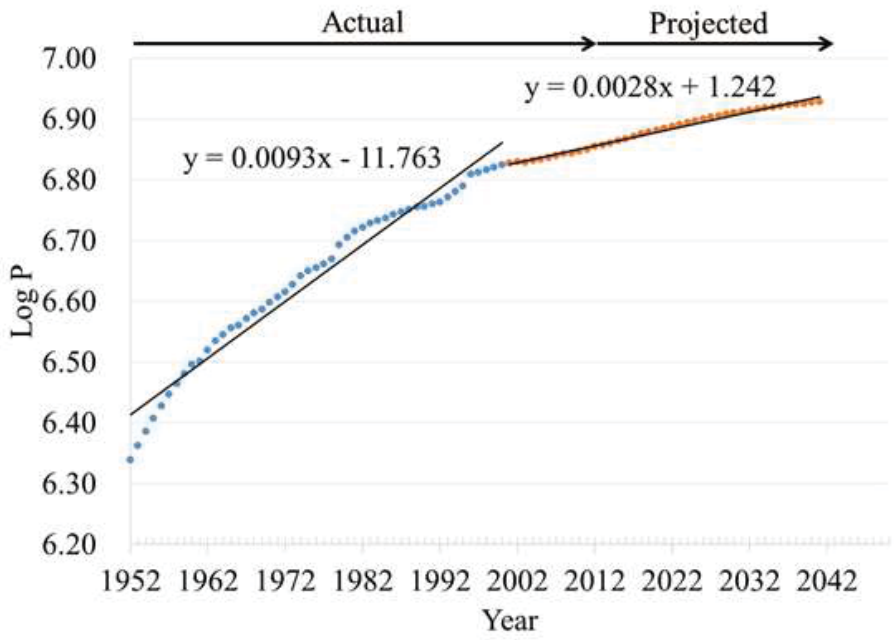

Fig. 4. *Logarithm of Hong Kong population (log P). The blue (orange) dots represent data for 1952-2000 (2001-2041), with black lines being the corresponding trend. Data for the period 2012-2041 are projected values.*

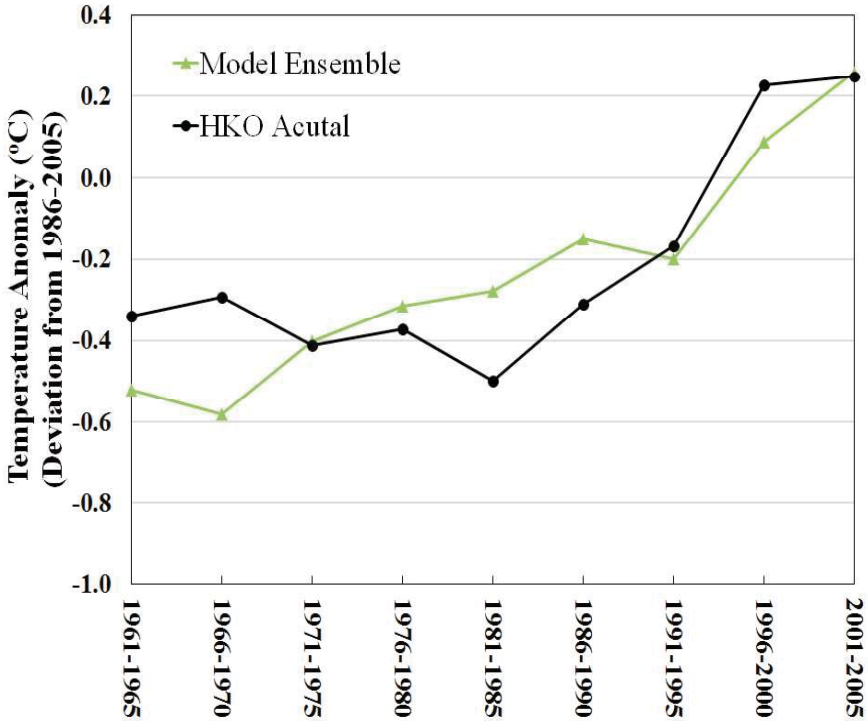

Fig. 5. *Anomaly of 5-year average temperature in Hong Kong (relative to the average temperature of 1986-2005). The black line is observations. The green line is the mean of downscaling results from the 25 CMIP5 models using the Set 1 predictor.*

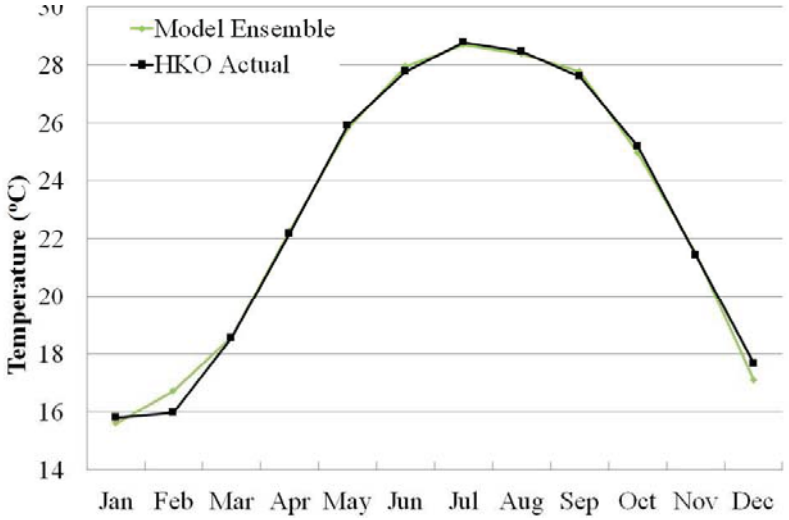

Fig. 6. *Annual cycle of temperature in Hong Kong during 1991-2005. Black is observations, green is the mean of downscaling results from the 25 CMIP5 models using the Set 1 predictor.*

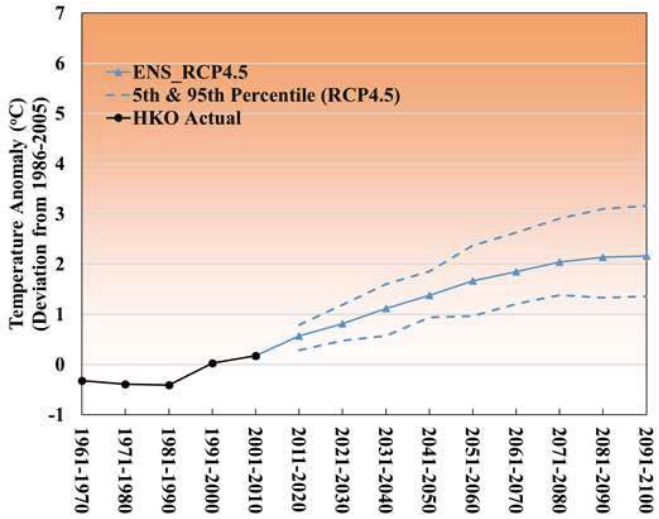

Fig. 7. *Projected decadal temperature anomaly (relative to the 1986-2005 average) of Hong Kong in the 21st century under the RCP4.5 scenario. The black line is actual observations; the solid blue line is the ensemble mean; and the dashed lines are the 5th and 95th percentiles of the ensemble.*

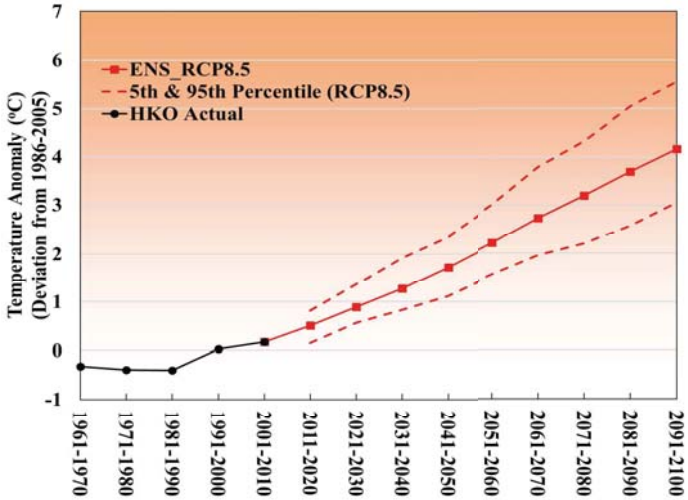

Fig. 8. *Same as Fig. 7, but for the RCP8.5 scenario. Projections indicated in red.*

Appendix

The same methodology presented in this paper is applied to RCP2.6 and RCP6.0. Models used for RCP2.6 and RCP6.0 are listed in Table A1. Fig. A1 (A2) shows the projected temperature change in Hong Kong for the 21st century under the RCP2.6 (RCP6.0) scenario. For the RCP2.6 (RCP6.0) scenario, the ensemble mean of the temperature rise reaches 1.3 °C (2.6 °C) in 2091-2100, with a likely range of 0.7 - 2.2 °C (1.8 - 3.6 °C).

				Resolution		Availability	
	Model	Center	Country	Latitude	Longitude	RCP2.6	RCP6.0
M2	BCC-CSM1-1	BCC	China	~ 2.8	2.8125	*	*
M3	BNU-ESM	BNU	China	~ 2.8	2.8125	*	
M4	CanESM2	CCCma	Canada	~ 2.8	2.8125	*	
M5	CCSM4	NCAR	USA	~0.94	1.25	*	*
M7	CSIRO-Mk36	CSIRO	Australia	~1.86	1.875		*
M8	FGOALS_g2	IAP	China	~ 2.8	2.8125	*	
M9	GFDL-ESM2G	NOAA GFDL	USA	~2	2.5	*	*
M10	GFDL-ESM2M	NOAA GFDL	USA	~2	2.5		*
M11	GISS-E2-H	NASA GISS	USA	2	2.5	*	*
M12	GISS-E2-R	NASA GISS	USA	2	2.5		*
M13	HadGEM2-AO	NIMR KMA	South Korea	1.25	1.875	*	*
M15	HadGEM2-ES	UKMO Had	UK	1.25	1.875	*	*
M17	IPSL-CM5A-LR	IPSL	France	~1.88	3.75	*	*
M18	IPSL-CM5A-MR	IPSL	France	~1.27	2.5	*	*
M20	MIROC5	MIROC	Japan	~1.4	1.40625	*	*
M21	MIROC-ESM	MIROC	Japan	~ 2.8	2.8125	*	*
M22	MIROC-ESM-CHEM	MIROC	Japan	~ 2.8	2.8125	*	*
M23	MRI-CGCM	MRI	Japan	~1.12	1.125	*	*
M24	Nor-ESM1-M	NCC	Norway	~1.88	2.5	*	*
M25	Nor-ESM1-ME	NCC	Norway	~1.88	2.5	*	*

Table A1. Details of the CMIP5 models used in this study for RCP2.6 and RCP6.0

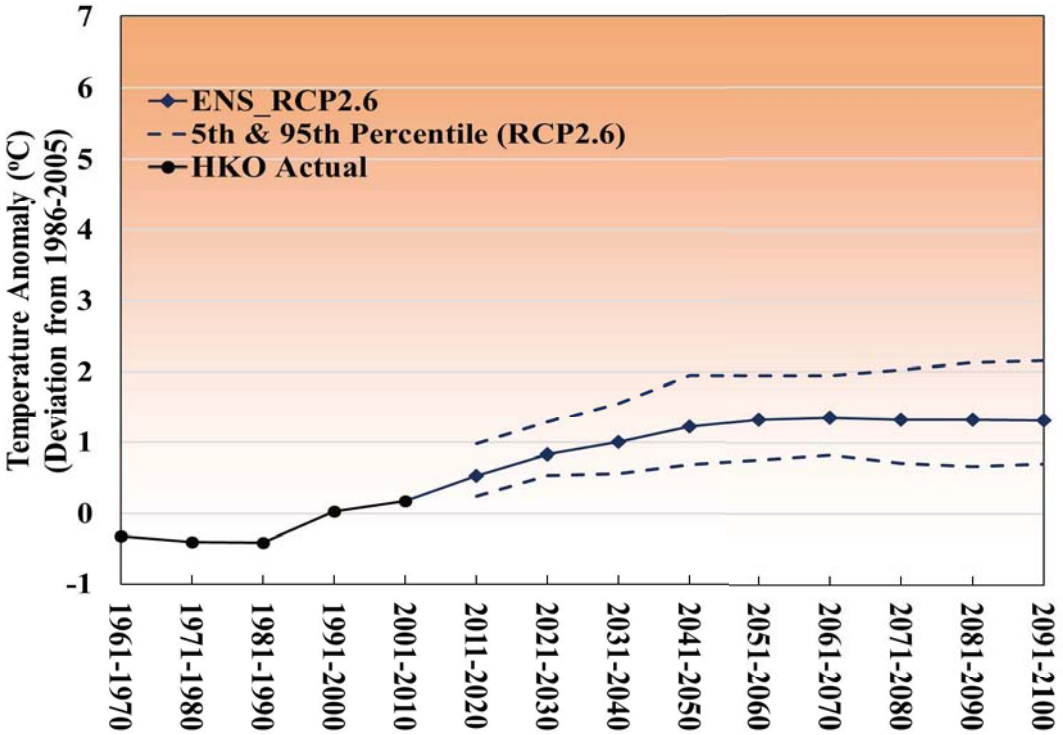

Fig. A1. Same as Fig. 7, but for the RCP2.6 scenario.

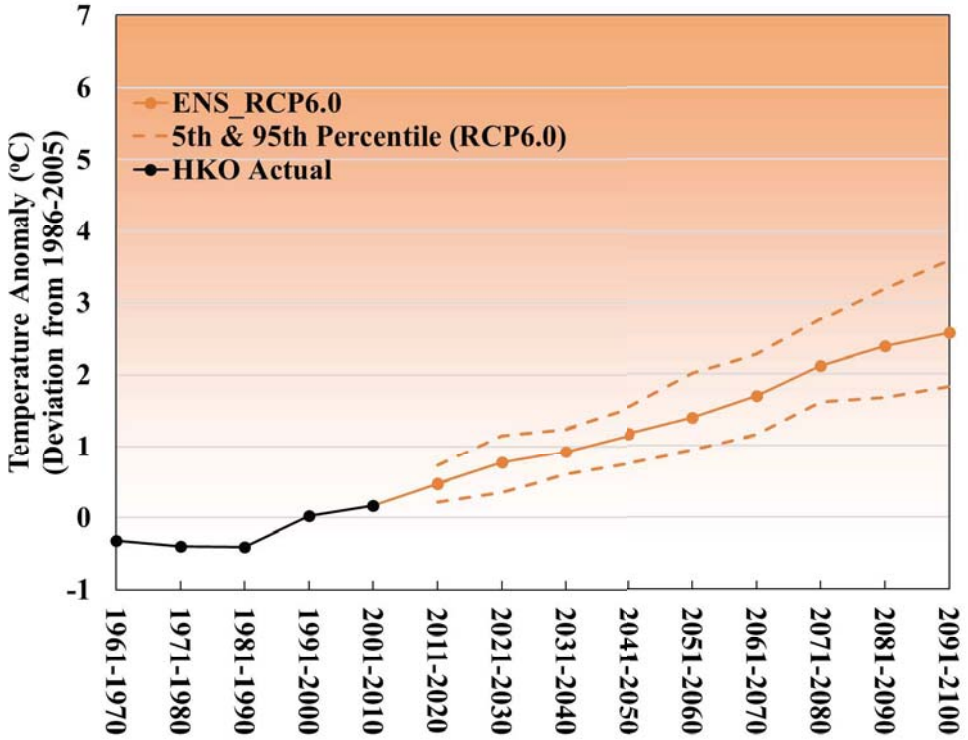

Fig. A2. Same as Fig. 7, but for the RCP6.0 scenario.

Latitudinal position of the East Asian trough and its modulation on winter temperatures over Southeast Asia

Marco Yu Ting Leung and Wen Zhou
School of Energy and Environment
City University of Hong Kong

Abstract

This study investigated the variations of East Asian winter monsoon (EAWM) and midlatitude atmospheric circulation concurrent with different latitudinal position of the East Asian trough (EAT). Through the regression analysis, we found that the latitudinal positions of the rising and sinking branches of the midlatitude zonal cell in the Western and Central Pacific vary according to that of the EAT. The changes in the cell induces the changes in the pressure systems in the lower troposphere including the southward displacement of the Aleutian low and weakened meridional pressure gradient over the Siberian high. This alters the path of cold air intrusion and contributes to the temperature anomalies in the low troposphere over East Asia.

1. Introduction

East Asian trough (EAT) is the stationary trough located at the midtroposphere over the midlatitude Western Pacific all the year round. It demonstrates the strongest intensity in boreal winter and weakest intensity in boreal summer. According to early studies, the EAT is one of the dominant climate systems to the East Asian winter monsoon (EAWM) [1,2,3]. Due to the strong geostrophic balance in the midlatitudes, air parcel propagates southeastward at the western and northeastward at eastern EAT. The southward (northward) transportation of the air parcel leads to the sinking (rising) motion at the western (eastern) part of the EAT. Hence, the EAT shows a strongly coupling with the surface pressure systems including the Siberian high and the Aleutian low [4,5]. The rising and sinking motions at the eastern and western EAT are also classified as two branches of the midlatitude zonal cell [6]. This illustrate that the EAT is important component of the EAWM and the midlatitude circulation.

To investigate the variations of the EAT, different characteristics are investigated in previous studies including strength and latitudinal and longitudinal positions of the trough [3]. It is noted that the variation of Southeast Asian winter temperature is close related to the latitudinal position of the EAT. However, the strength and longitudinal position of the EAT shows weak relationship with Southeast Asian winter temperature. In order to understand the interannual variation of Southeast Asian winter climate, we need to clarify the linkage between circulation and latitudinal position of the EAT. Therefore, this study is carried out to investigate their linkage.

This study comprises 4 sections. This section is introduction. Section 2 describes the data and methodology utilized. The result of the study is illustrated in section 3. A brief summary is presented in section 4.

2. Data and methodology

The study period of this study is from 1979 to 2014. Winters season is defined as December to February (DJF). We used the ERA-interim reanalysis as proxy of observation [7]. Different parameters of this reanalysis are utilized including geopotential (ϕ), air temperature (T), vertical velocity (), zonal wind (U) and meridional wind (V). The horizontal resolution of the reanalysis is 2.5˚×2.5˚. Pressure levels 500 and 850 hPa are selected to investigate the modulation of the midtroposphere EAT to the lower level winter climate over Southeast Asia.

The climatology of geopotential height, Z= ϕ/9.8, is shown in Fig. 1a. The geopotential height over the trough is remarkably lower than the adjacent region at the same latitude. To evaluate the variation of latitudinal position of the EAT, we follow the method in previous studies [3]. We applied the empirical orthogonal function analysis on the geopotential height, Z= ϕ/9.8, over the region around the EAT (30˚ to 65˚N and 120˚ to 160˚E) at the pressure level of 500 hPa. The spatial pattern of first EOF and its corresponding time series are displayed in Fig. 1b and c. The EOF pattern shows negative values at the south and positive at the north. So, the winters with positive value in the time series represent the EAT positioning to the south of its climatological position and vice versa for the winters with negative value.

3. Result

To depict the modulation of the EAT on the mid- and lower-tropospheric circulation, regression analysis is employed. The regressions of vertical velocity at 500 hPa and geopotential height at 850 hPa onto the standardized PC1 are delineated in Fig. 2b and d. The climatological mean of the vertical velocity shows a strong sink motion at the western and moderate rising motion at the eastern EAT (Fig. 2a). When the EAT locates to the south of its climatological position, the sinking motion at the western and rising motion at the eastern EAT also demonstrate remarkable southward displacements (Fig. 2b). This suggests the vertical motions over the midlatitude Western and Central Pacific change concurrent with the latitudinal position of the EAT. Therefore, the latitudinal position of the EAT can significant influence that of the rising and sinking branches of the midlatitude zone cell.

In addition, it is worth noting that the rising motion at the eastern EAT coincides with the Aleutian low in the lower troposphere (Fig. 2a and c). The rising motion at the eastern EAT contributes to the low pressure and convergent flow at the lower troposphere and high pressure and divergent flow at the upper troposphere. Hence, the southward displacement of the rising motion at the eastern EAT leads to a southward displacement of the Aleutian low (Fig. 2d). Aside from the displacement of the Aleutian low, significant positive values can be found to the north of the Siberian high (Fig. 2d). This weakens the meridional pressure gradient in the lower troposphere over the upstream regions of East Asia. Consequently, both of the Siberian high and the Aleutian low are also affected by the latitudinal position of the EAT.

In this study, the changes of wind and temperature in the lower troposphere are also investigated. Their climatological mean and regressions onto standardized PC1 are presented in Fig. 3. The regression of temperature at 850 hPa shows significant negative values over the most parts of Southeast Asia (Fig. 3b). On the other hand, positive values can be found over Northeast Asia. The anomalous temperatures over East Asia is caused by the anomalous horizontal wind in the lower troposphere as shown in Fig. 3d. Strong cyclonic flow exits over the midlatitude Western Pacific (Fig. 3d). It carries warm oceanic air westward to the regions around the Okhotsk Sea and cold inner-continence air southeastward to the subtropical western Pacific and southward to the coastal regions of South China (Fig. 3a and d).

By comparing the regression of wind with its climatological mean (Fig. 3c and d), we found that the westerly component of wind to the north of 40˚N over East Asia and the Western Pacific is suppressed and northerly component is enhanced. This illustrates a change in the path of cold air in conjunction with the latitudinal variation of the EAT. The change in the path of cold air is consistent with the changes in pressure gradient in the lower troposphere. The suppression of the westerly component is resulted from the southward displacement of the Aleutian low and the weakened meridional pressure gradient over the Siberian high (Fig. 2d). The enhanced northerly wind is caused by steeper than normal zonal gradient due to the southward displacement of the Aleutian low.

4. Summary

In this study, the modulation of the latitudinal position of the EAT on the midlatitude circulation and EAWM is documented. We found that the latitudinal positions of the rising and sinking branches of the midlatitude zonal cell in the Western and Central Pacific vary along with that of the EAT. The southward displacement of the zonal cell contributes to changes in the lower troposphere pressure systems including the Siberian high and the Aleutian low. This alters the path of cold air and results in temperature in the lower troposphere. Based on the statistical analysis of this study, the latitudinal location of the EAT plays an important role in variations of the EAWM and midlatitude circulation.

References

[1.] Wang, L., W. Chen, W. Zhou, and R. Huang, 2009: Interannual variations of East Asian trough axis at 500 hPa and its association with the East Asian winter monsoon path. *J. Climate.*, **22**, 600-614.

[2.] Leung, M. Y.-T., and W. Zhou, 2015: Vertical structure, physical properties, and energy exchange of the East Asian trough in boreal winter. *Clim. Dyn.*, **45**, 1635-1656.

[3.] Leung, M. Y.-T., and W. Zhou, 2015: Variation of circulation and East Asian climate associated with anomalous strength and displacement of the East Asian trough. *Clim. Dyn.*, **45**, 2713-2732.

[4.] Ding, Y., and T. N. Krishnamurti, 1987: Heat budget of the Siberian high and the winter monsoon. *Mon. Wea. Rev.*, **115,** 2428-2449.

[5.] [5] Zhang, Y., K. R. Sperber, and J. S. Boyle, 1997: Climatology and interannual variation of the East Asian winter monsoon: results from the 1979-95 NCEP/NCAR reanalysis. *Mon. Wea. Rev.*, **125,** 2605-2619.

[6.] [6] Wang, C., 2002: Atmospheric circulation cells associated with the El Niño–Southern Oscillation. *J. Climate,* **15,** 399-419.

[7.] [7] Dee, D. P., and Coauthors, 2011: The ERA-Interim reanalysis: Configuration and performance of the data assimilation system. *Quart. J. Roy. Meteor. Soc.*, **137,** 553-597.

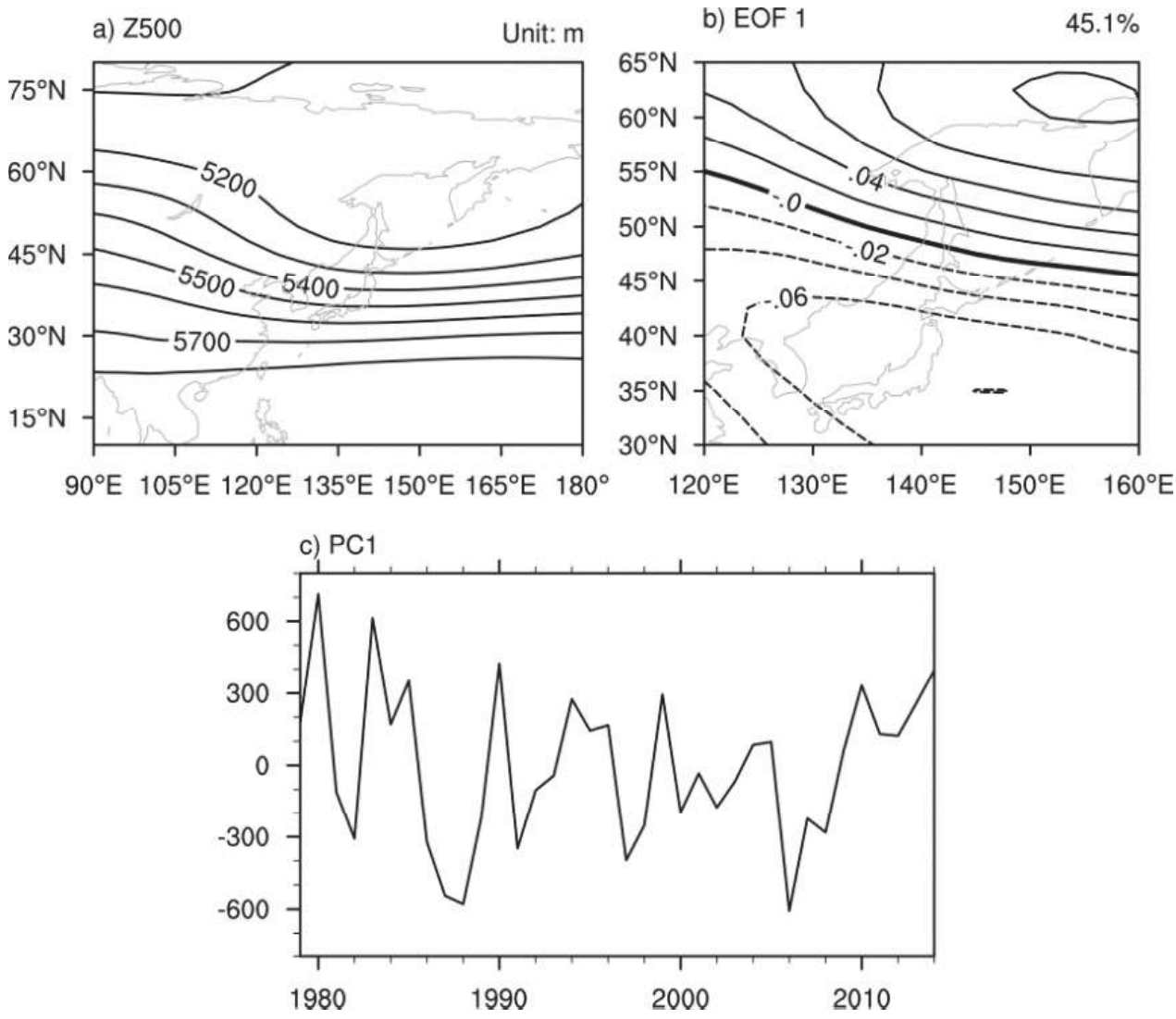

Fig. 1. (a) Climatology of geopotential height at 500 hPa (Z500). (b) The first EOF (EOF1) pattern of Z500. (c) The corresponding time series (PC1) of EOF1.

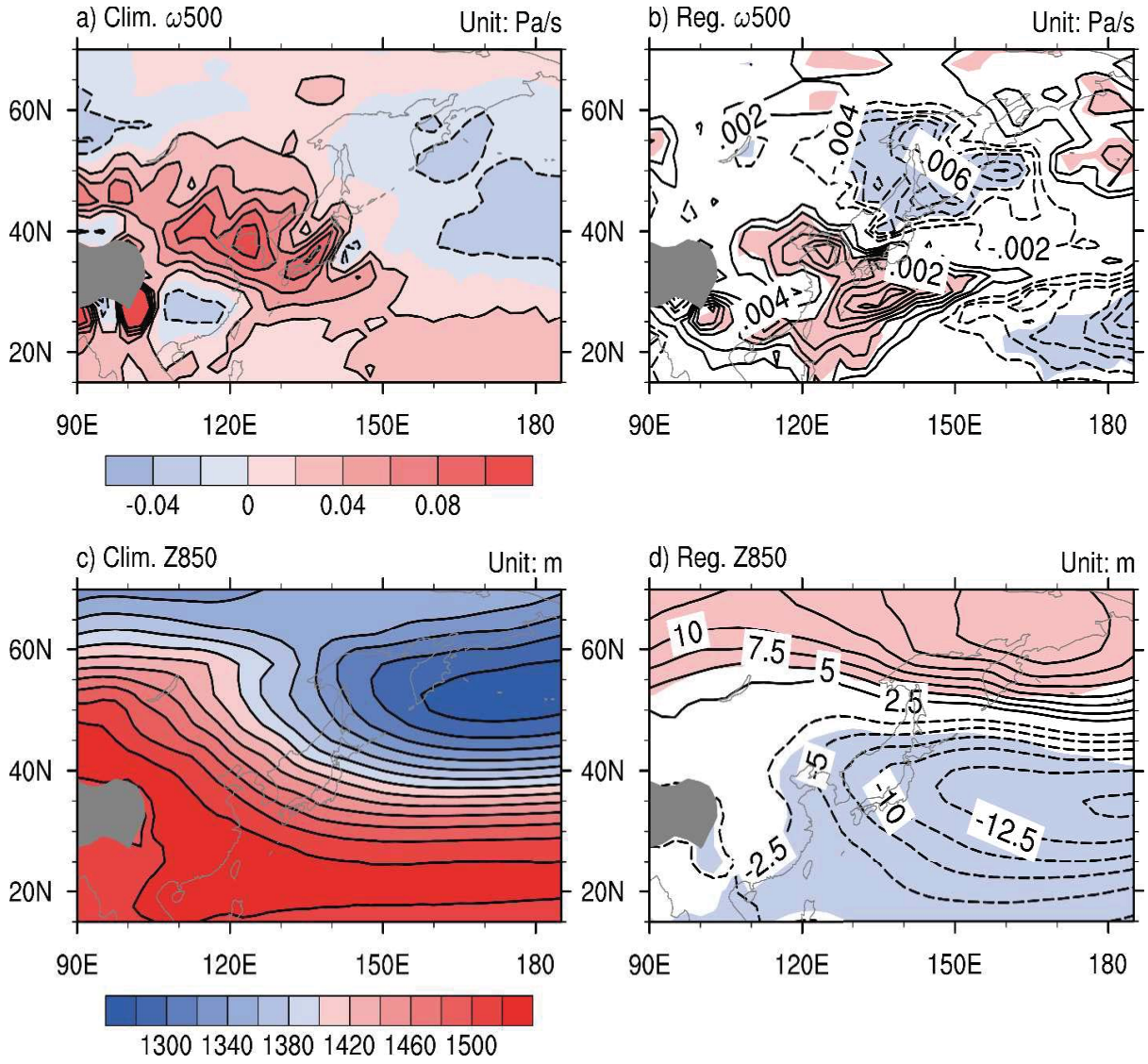

Fig. 2. (a) Climatological vertical velocity at 500 hPa (500). (b) Regression of 500 onto standardized PC1. (c) and (d) are similar to (a) and (b), but for geopotential height at 850 hPa (Z850). In (b) and (d), blue and red shading indicates the negative and positive values excess the 5% significance level. The values below the ground surface are shaded with gray color.

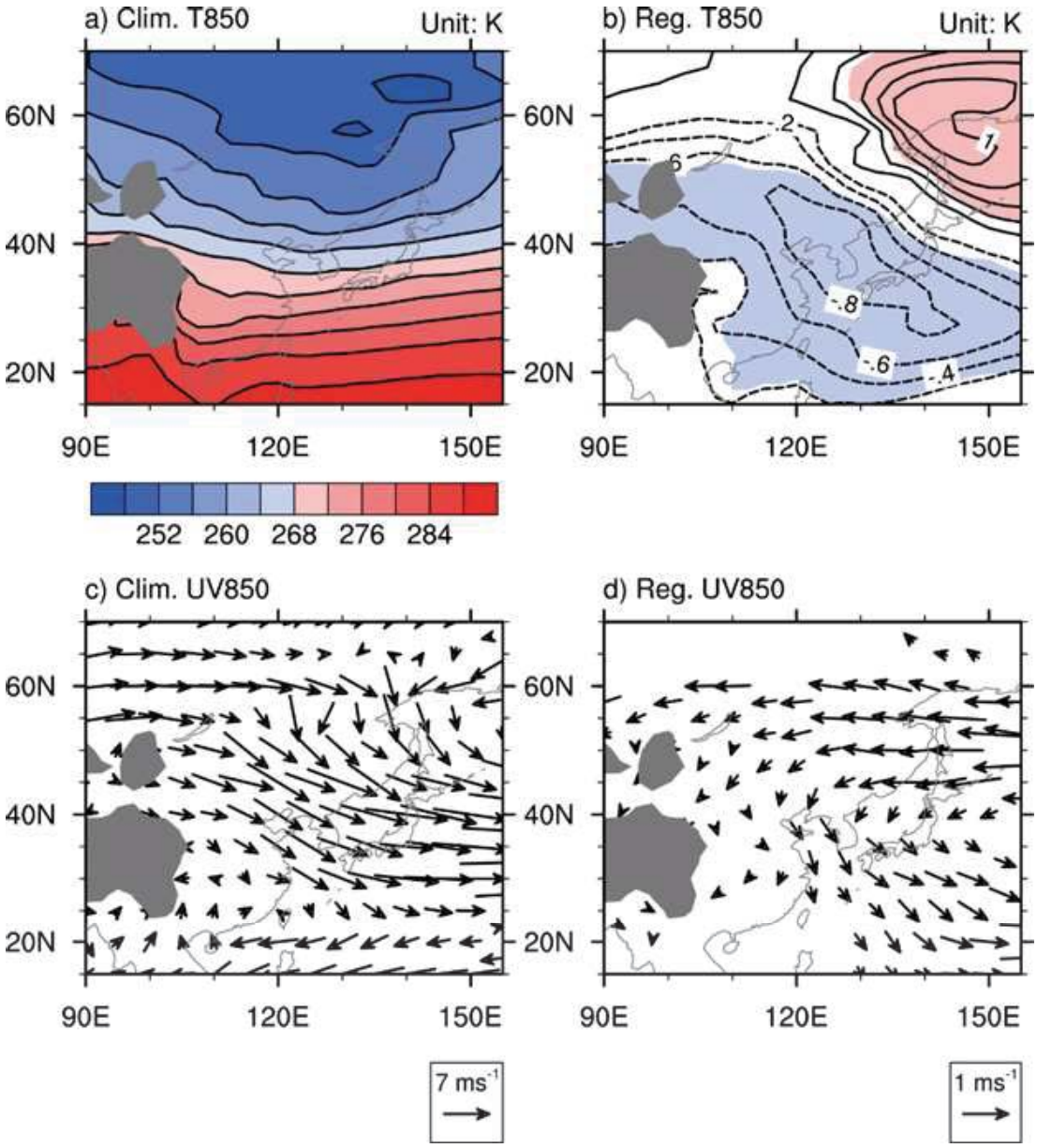

Fig. 3. (a) Climatological air temperature at 850 hPa (T850). (b) Regression of T850 onto standardized PC1. (c) and (d) are similar to (a) and (b), but for horizontal wind at 850 hPa (UV850). In (b), blue and red shading indicates the negative and positive values excess the 5% significance level. In (c), only the vectors excesses the 5% significance level are plotted. The values below the ground surface are shaded with gray color.

Winds That Help a City to Breathe

Edwin S T Lai, T C Lee, and Y H Lau
Hong Kong Observatory

Abstract

The microclimate of wind is an important consideration in planning and building a sustainable city. The Hong Kong Observatory has been conducting meteorological observations in Hong Kong since 1884. The establishment of the automatic weather station (AWS) network in the mid-1980s further expanded the spatial coverage and improved the temporal resolution of wind observations in Hong Kong. This study aims to provide a concise review of the characteristics of the wind climate of Hong Kong from a seasonal and regional perspective using AWS data from the last three decades. Wind trends over different parts of Hong Kong are analysed and potential applications of the results are discussed, including implications for sustainable development.

1. INTRODUCTION

Located on the eastern side of the Pearl River Estuary of South China, Hong Kong has a subtropical climate with background winds dominated by the monsoon systems most of the time. In winter, the northeast monsoon brings cold and dry continental air to Hong Kong. In summer, Hong Kong is hot and humid largely due to the maritime air associated with the southwest monsoon. There are on average six tropical cyclones that come within 500 km of Hong Kong each year, occasionally bringing high winds to the territory. With a land area of about 1,000 km2 and a complex topography, Hong Kong has a lot of variation in its shelter from and exposure to winds over different parts of the territory. With rapid urbanization over the past 50 years or so, land use changes and dense building development have further complicated the microclimate and local wind flow in and around the city.

The Hong Kong Observatory has been conducting meteorological measurements at Tsim Sha Tsui in Hong Kong since 1884, with wind measurement being one of the earliest meteorological observations. Anemometer stations were progressively set up at different locations in the territory from the 1950s to the 1970s, such as Waglan Island, the Kai Tak Airport, Cheung Chau, Star Ferry Pier (Kowloon), King's Park, and Tai O (Chen, 1975). The establishment of the automatic weather station (AWS) network in the mid-1980s further expanded the spatial coverage and improved the temporal resolution of wind observations in Hong Kong (Wong *et al.*, 1984; Lui, 1991). This study reviews the characteristics of the wind climate of Hong Kong from a seasonal and regional perspective using AWS data from the past three decades. It also focuses on a number of selected conventional anemometer stations to study the long-term variation in the background and urban wind environment of Hong Kong.

The data and analysis methods are explained in Section 2, and the analysis results are presented in Section 3. The microclimate of wind is an important consideration in planning and building a sustainable city, and potential applications of wind climate information are briefly discussed in Section 4. Finally, a summary of the findings is provided in Section 5.

2. DATA AND METHODOLOGY

Wind speed and direction data from 21 AWSs with continuous wind measurements

for 20 years or more were used in this study. Hourly 60-minute mean wind speed data from these 21 AWSs were computed to obtain the monthly, seasonal, and annual mean wind speeds. The four seasons of spring, summer, autumn, and winter refer respectively to the months of March to May (MAM), June to August (JJA), September to November (SON), and December to February (DJF). Hourly data with annual availability less than 80% were not used in calculating the mean and the trend.

The prevailing wind direction was obtained from the frequency distribution of wind direction by applying a 5-term binomial weighting factor (1-4-6-4-1) (Yeung *et al.*, 1986). For trend analysis, linear regression lines were fitted to the parameters by least squares. A two-tailed t-test was applied to evaluate the statistical significance of the trends at the 5% significance level.

For long-term trend analysis, the data period for Waglan Island, Kai Tak (Southeast), and King's Park was extended back to 1968 using conventional wind observation data. Since hourly observations were not available at King's Park during the conventional station era, and because we wanted to compare like with like, the 12-hourly (at 00 and 12 UTC) 10-minute wind speed data from Waglan Island, Kai Tak (Southeast), and King's Park from 1968 to 2013 were used for the comparison of long-term trends.

The station codes, anemometer elevations, data periods, and locations are listed in Table 1. The topography of Hong Kong and location of the stations are shown in Figures 1 and 2.

3. RESULTS

The annual and seasonal mean wind speeds and prevailing wind directions of the 21 AWSs are summarized in Table 2 in descending order of annual mean wind speed. The annual wind rose diagrams of the stations are also overlaid on the topography map of Hong Kong in Figures 1 and 2 for reference.

2.1. Wind speed

Tai Mo Shan, Green Island, Tate's Cairn, Waglan Island, and Cheung Chau have higher average wind speeds, ranging from 5 ms^{-1} to 7 ms^{-1}. These stations are all on high ground or offshore islands with good exposure to the background flow. The average wind speed of stations within the Victoria harbour (Star Ferry, Kai Tak (Southeast)) or the shoreline (Sha Lo Wan, Tai Mei Tuk, and Lau FauShan) are generally between 3 ms^{-1} and 4 ms^{-1}. Stations in the built-up areas (e.g., Hong Kong Observatory and Tseung Kwan O), inland (Ta Kwu Ling), or with significant sheltering terrain nearby (e.g., Tuen Mun and Sha Tin) have relatively low wind speeds of less than 3 ms-1. The average wind speed of Ping Chau is the lowest and may be partly attributed to the shelter it receives to the east and north.

For seasonal variation, the background flow represented by Waglan Island, Tai Mo Shan, and Tate's Cairn shows that the mean wind speed in summer tends to be slightly lower than that in other seasons. However, no consistent tendency in the seasonal difference in wind speed is observed for other stations.

2.2. Prevailing wind direction

While easterly is the predominant direction for most of the stations, topographic effects are also prominent at Tuen Mun, Shell Oil Depot, and Sai Kung. As depicted in Table 2 and Figures 1 and 2, seasonal changes in wind direction are well marked at exposed stations like Tai Mo Shan, Waglan Island, Cheung Chau, etc. At Waglan Island, the wind direction changes from the northeast quadrant in winter to the southwest quadrant in summer. Inside the Victoria harbour, east to southeasterly winds prevail at Star Ferry and Kai Tak (Southeast) for most of the year due to a channelling effect.

2.3. Trend analysis

Table 3 shows the trends of the annual mean wind speeds of the AWSs in the last two to three decades. Apart from Sha Tin and Green Island, all stations have either no significant trend or a decreasing trend in wind speed during the study period. The general decrease in wind speed is consistent with a slight decreasing trend in the background flow as observed at exposed stations like Tai Mo Shan, Waglan Island, and Cheung Chau. For Sha Tin and Green Island, the increasing trends are associated mainly with relatively high wind speeds in the past 10 years or so, which may be related to other site-specific factors such as nearby environmental changes since the mid-1990s. Future studies of the microclimate will be required to identify the possible causes.

To study the urbanization effect on local wind speeds, long-term data at Waglan Island, Kai Tak (Southeast), and King's Park since 1968 were analyzed by combining the 12-hourly (at 00 and 12 UTC) 10-minute mean wind speed data from the conventional and AWS eras. For reference, similar 12-hourly AWS data measured at the Hong Kong Observatory at Tsim Sha Tsui since 1984 were also plotted alongside for comparison. As shown in Figure 3, in the past 45 years, while no significant trend in the annual wind speed could be detected at Waglan Island, a decreasing trend was found in the other three urban stations, in particular at the Hong Kong Observatory and King's Park. Rapid and dense building development in the past few decades effectively increased the roughness of the surface underlying the atmosphere and exerted a drag on the low-level air flow.

4. IMPLICATIONS FOR SUSTAINABLE DEVELOPMENT

4.1 Urban planning

Since the Severe Acute Respiratory Syndrome episode in 2003, the planning community in Hong Kong has included the wind factor in urban design to optimize air ventilation. The Planning Department has set up guidelines to assess and regulate the impact of potential city, community, and building developments on local air ventilation (HPLB & ETWB, 2006; Ng, 2009). By analysing and evaluating climate wind data together with different geometric and urban development data (e.g., land use, greening, building density, topography), "Urban Climatic Maps" have been drawn up by the Chinese University of Hong Kong to divide the territory into different urban climate zones, each with recommended planning and development actions (Ng *et al.*, 2011; Ren *et al.*, 2013).

4.2 Air quality monitoring and assessment

Wind flow is one of the key elements affecting the air quality in Hong Kong. Good understanding of the regional wind climate (monsoon and tropical cyclones) and local wind patterns (land sea breezes and katabatic winds) provides a useful scientific basis for monitoring and predicting the transport of the pollutants (Koo *et al.*, 1984; Lam and Lau, 2005). In-situ wind data and other meteorological observations (e.g., temperature, atmospheric stability, sunshine, etc.) are essential inputs for computer models operated by the Environmental Protection Department to forecast the air quality in Hong Kong in the next 48 hours (Fung, 2006). Moreover, site-specific wind flow information is commonly used in dispersion models for odour management and impact assessment of waste management activities.

4.3 Infrastructure design

Strong and gusty winds can be destructive. The design of safe buildings and other infrastructure against extreme winds due to tropical cyclones or other severe weather phenomena has always been one of the prime concerns of the engineering community. Data on extreme winds in Hong Kong since the 1950s have been used for

the establishment of the Code of Practice on Wind Effects (BD, 2004) and Port Work Design Manual (CEDD, 2002).

4.4 *Wind power potential*

Analyses of the long-term wind data measured by the Observatory provide information on the potential of wind energy resources in Hong Kong (Wong and Kwan, 2002; Lee and Mok, 2010). Such information has been found useful for relevant feasibility and site selection studies (CLP, 2006; HKE, 2010).

5. SUMMARY

Wind data gathered by the anemometer networks of the Observatory reveal large variations in the wind speeds and prevailing wind directions over different parts of the territory. Stations on high ground and offshore islands generally have a relatively higher wind speed than inland stations or those enclosed by complex terrain. While there are distinctive seasonal variations in wind direction at well-exposed stations, the channelling effect within the harbour results in a dominance by easterly winds all year round. Moreover, the long-term trend study shows a significant decreasing trend in wind speed at King's Park, the Hong Kong Observatory, and Kai Tak that can be attributed to nearby urban development in the past decades.

References

BD, Codes of Practice, Design Manuals and Guidelines http://www.bd.gov.hk/english/documents/index_crlist.html

CEDD, 2002: Port Work Design Manual http://www.cedd.gov.hk/eng/publications/ceo/pwdm.htm

Chen, T.Y., 1975: Comparison of surface winds in Hong Kong, Royal Observatory Hong Kong, Technical Note No. 41.

CLP, 2006: Hong Kong Offshore Wind Farm in Southeastern Waters. https://www.clp.com.hk/offshorewindfarm/home.html

Fung, C., 2006: The challenges of modelling air quality in Hong Kong, Symposium of Science in Public Services, Science Museum, Hong Kong, 27 April 2006.

HKE, 2010: Development of an Offshore Wind Farm in Hong Kong, EIA Study, Executive Summary. http://www.epd.gov.hk/eia/register/report/eiareport/eia_1772009/PDF/0088440_Executive%20Summary_v6.pdf

HPLB & ETWB, 2006: Air Ventilation Assessment, Technical Circular No. 1/60.

Koo, E., C.M. Tam and W.L. Chang, 1984: Air pollution meteorology research in Hong Kong, 5th Clean Air Conference, Melbourne, Australia, 5-11 May 1984.

Lam, C.Y. and K.H. Lau, 2005: Scientific background of haze and air pollution in Hong Kong, The 13th Annual Conference of Hong Kong Institution of Science, Hong Kong China, 29 October 2005.

Lee, B.Y. and H.Y. Mok, 2010: Potential of wind and solar energy in Hong Kong, Symposium on E-Management - Challenges and Opportunities, Hong Kong, 28 May 2010.

Lui, W.H., 1991: Preliminary analysis of wind data recorded by automatic weather stations in Hong Kong, Royal Observatory Hong Kong, Technical Note (Local) No. 59.

Ng, E., 2009: Air Ventilation Assessment for High Density City - An Experience from Hong Kong, The Seventh International Conference on Urban Climate, 29 June - 3 July 2009, Yokohama, Japan.

Ng, E., C. Yuan, L. Chen, C. Ren, J.C.H. Fung, 2011: Improving the wind environment in high-density cities by understanding urban morphology and surface roughness: A study in Hong Kong, Landscape and Urban Planning 101, 59–74.

Ren, C., E. Ng, K. Lutz and J. Fung, 2013: The application of wind information to the urban planning of Hong Kong, PLEA 2013 - 29th Conference, Sustainable Architecture for a Renewable Future, Munich, Germany, 10-12 September 2013.

Wong, M.C., K.H. Yeung and L.K. Yau, 1984: An automatic weather station (AWS) network in Hong Kong, The WMO Technical Conference on Instruments and Cost-effective Meteorological Observations (TECIMO), 24-28 September 1984.

Wong, M.S. and W. K. Kwan, 2002: Wind statistics in Hong Kong in relation to wind power, Hong Kong Observatory Technical Note (Local) No. 77, 29 pp.

Yeung, K.H., K.K. Ng and L.K. Yau, 1986: A solar-powered automatic weather station, Royal Observatory Hong Kong, Technical Note No. 75.

Table 1 List of stations, elevations, and data periods used in the study.

Station Name	Station Code	Anemometer elevation (metres boveMSL)	Data Period	
			Automatic	Conventional
Hong Kong Observatory	HKO	74	1984-2013	--
Sha Tin	SHA	16	1984-2013	--
Lau Fau Shan	LFS	67	1985-2013	--
Ta Kwu Ling	TKL	50	1985-2013	--
Tai Mo Shan	TMS	966	1987-2013	--
Tate's Cairn	TC	587	1987-2013	--
Wong Chuk Hang	HKS	30	1989-2013	--
Waglan Island	WGL	83	1989-2013	1968-1989
Green Island	GI	107	1989-2013	--
Tseung Kwan O	JKB	52	1991-2013	--
Cheung Chau	CCH	99	1992-2013	--
King's Park*	KP	90	1992-2013	1968-1992
Ping Chau	EPC	39	1993-2013	--
Tai Mei Tuk	PLC	71	1993-2013	--
Sha Lo Wan	SLW	71	1993-2013	--
Sai Kung	SKG	32	1993-2013	--
Tap Mun	TAP	35	1993-2013	--
Kai Tak (Southeast)	KTSE	16	1998-2013	1968-1998
Tuen Mun	TUN	69	1987-2013	--
Star Ferry (Kowloon)	SF	18	1987-2013	--
Shell Oil Depot	SHL	43	1987-2013	--

* The anemometer at King's Park AWS was relocated (within the station) to a higher elevation in 1996.

Table 2 *Summary of annual and seasonal mean wind speeds (m/s) and prevailing directions (degrees) at the selected AWS.*

Station Code	Annual		Spring (MAM)		Summer (JJA)		Autumn (SON)		Winter (DJF)		Data Period
	Speed	Dir	Speed	Dir	Speed	Dir	Speed	Dir	Speed	Dir	
TMS	7.0	110	7.0	110	6.9	200	7.3	90	6.6	110	1987-2013
WGL	6.3	70	5.8	70	5.7	230	6.9	80	6.9	60	1989-2013
TC	6.2	100	6.3	100	5.4	180	6.5	100	6.6	100	1987-2013
GI	5.9	70	6.2	70	5.2	190	5.9	70	6.2	70	1989-2013
CCH	5.1	100	4.7	100	5.0	200	5.5	100	5.0	360	1992-2013
KTSE	3.7	110	3.8	110	3.6	130	3.7	100	3.6	110	1984-2013
LFS	3.5	80	3.6	80	3.7	140	3.4	80	3.4	70	1985-2013
PLC	3.4	50	3.2	50	3.5	260	3.9	40	3.2	40	1993-2013
SLW	3.4	90	3.8	80	3.6	220	3.3	90	3.1	80	1993-2013
SF	3.3	100	3.5	100	3.1	100	3.3	100	3.2	100	1987-2013
SKG	2.8	20	2.4	180	2.7	180	3.3	10	2.9	20	1993-2013
TAP	2.8	120	2.6	120	2.4	120	3.0	120	3.0	350	1993-2013
HKO	2.6	90	2.7	90	2.5	260	2.7	90	2.5	90	1984-2013
SHL	2.6	120	2.8	110	2.7	150	2.3	120	2.4	110	1987-2013
KP	2.4	110	2.5	110	2.3	110	2.5	100	2.3	100	1992-2013
HKS	2.4	100	2.3	110	2.2	110	2.7	90	2.3	90	1989-2013
TUN	2.4	160	2.4	160	2.5	160	2.3	30	2.2	30	1987-2013
TKL	2.2	110	2.5	110	1.8	110	2.1	110	2.3	110	1985-2013
SHA	2.1	90	2.2	90	2.3	220	2.1	20	2.1	30	1984-2013
JKB	2.0	20	1.8	20	1.9	200	2.1	20	2.0	20	1991-2013
EPC	1.3	80	1.4	80	1.3	150	1.2	80	1.4	80	1993-2013

Table 3 *Trend analysis of the AWS annual mean wind speeds. The highlighted trends (blue for increasing and yellow for decreasing) are statistically significant at the 5% level.*

Station Code	Trend	Data Period
	Annual mean wind speed	
HKO	-0.16 ms-1/decade	1984-2013
SHA	+0.16 ms-1/decade	1984-2013
LFS	-0.08 ms-1/decade	1985-2013
TKL	-0.36 ms-1/decade	1985-2013
TMS	-0.23 ms-1/decade	1987-2013
TC	-0.06 ms-1/decade	1987-2013
HKS	-0.00 ms-1/decade	1989-2013
WGL	-0.10 ms-1/decade	1989-2013
GI	+0.37 ms-1/decade	1989-2013
JKB	-0.40 ms-1/decade	1991-2013
CCH	-0.13 ms-1/decade	1992-2013
KP	-0.11 ms-1/decade	1996-2013*
EPC	-0.45 ms-1/decade	1993-2013
PLC	-0.29 ms-1/decade	1993-2013
SLW	-0.42 ms-1/decade	1993-2013
SKG	-0.15 ms-1/decade	1993-2013
TAP	-0.35 ms-1/decade	1993-2013
KTSE	-0.34 ms-1/decade	1984-2013
TUN	+0.02 ms-1/decade	1987-2013
SF	+0.02 ms-1/decade	1987-2013
SHL	-0.39 ms-1/decade	1987-2013

* The anemometer at King's Park AWS was relocated (within the station) to a higher elevation in 1996

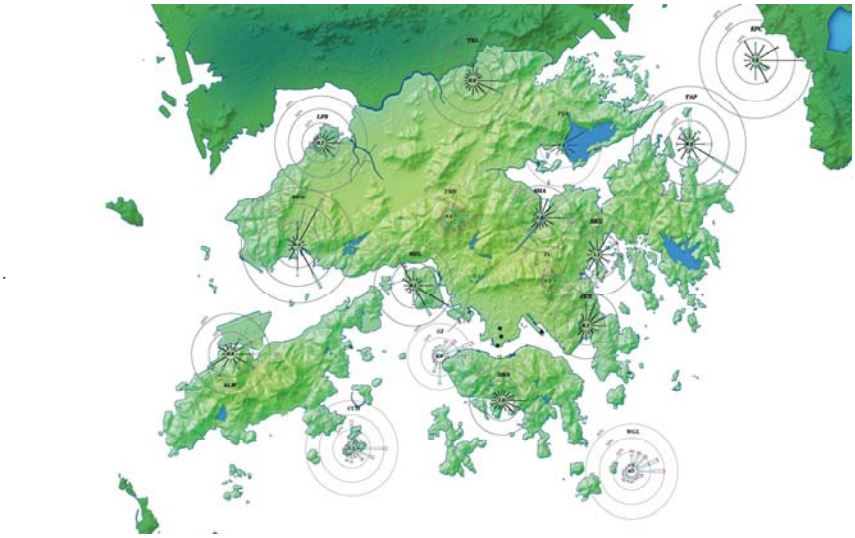

Figure 1 *Annual wind rose of automatic weather stations operating on or before 1993 (20 years or more).*

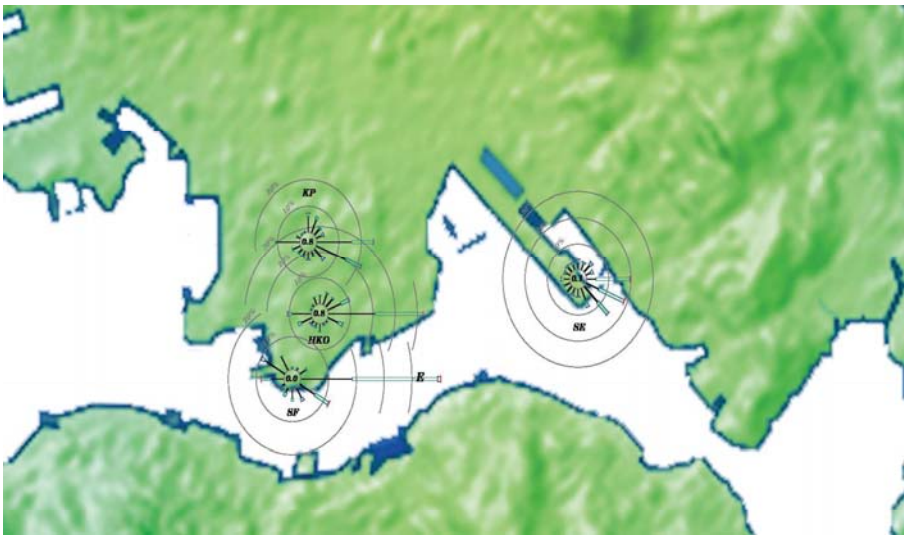

Figure 2 *Annual wind rose of the Hong Kong Observatory, Kai Tak (Southeast), Star Ferry, and King's*

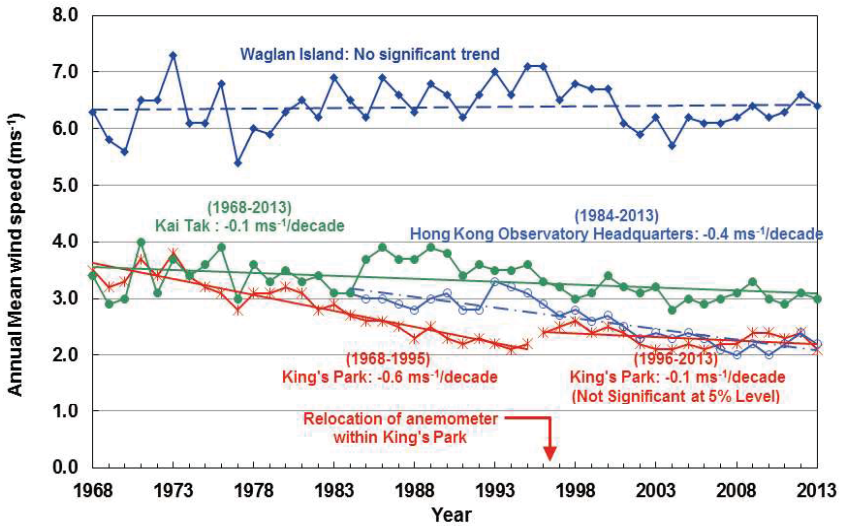

Figure 3 *Trends of the annual average of 12-hourly (at 00 and 12 UTC) 10-minute mean wind speeds at King's Park, Kai Tak, and Waglan Island from 1968 to 2013, as well as those at Hong Kong Observatory (since 1984).*

普及氣象科學講座系列：天災解碼 - 整合氣候變化拼圖

Popular Meteorological Science Lecture Series : Decoding Natural Disasters – Piecing Together the Climate Change Jigsaw Puzzle

參觀賽馬會氣候變化博物館

Visit to the Jockey Club Museum

香港氣象學會主辦，香港美術教育協會、香港天文台協辦
『齊抗天災』繪畫比賽

得獎名單 - 初級組

名次	姓名	學校
初級組 - 冠軍	秦朗	高主教書院小學部
初級組 - 亞軍	劉康妮	高主教書院小學部
初級組 - 季軍	何彥青	嘉諾撒聖方濟各學校
初級組 - 優異	洪紫程	高主教書院小學部
初級組 - 優異	莫承軒	天水圍官立小學
初級組 - 優異	盧欣妍	啟基學校
初級組 - 優異	盧卓言	啟基學校

冠軍 秦朗

亞軍 劉康妮

季軍 何彥青

『齊抗天災』繪畫比賽

得獎名單 - 高級組

名次	姓名	學校
高級組 - 冠軍	吳美璇	上水宣道小學
高級組 - 亞軍	何菁元	嘉諾撒聖方濟各學校
高級組 - 季軍	鄭凱軒	路德會梁鉅　小學
高級組 - 優異	陳暈婷	培正小學
高級組 - 優異	周朗恆	北角衛理小學
高級組 - 優異	馮啟軒	英華小學
高級組 - 優異	廖穎如	聖公會主愛小學

冠軍 吳美璇

亞軍 何菁元

季軍 鄭凱軒

初級組 - 優異

高級組 - 優異

HONG KONG METEOROLOGICAL SOCIETY

INFORMATION FOR CONTRIBUTORS TO THE BULLETIN

Technical or research articles, as well as reviews and correspondence of a topical nature are welcome. In general contributions should be short, although exceptions may be made by prior arrangement and at the sole discretion of the Editorial Board. Copyright of material submitted for publication remains that of the author(s). However, any previous, current, or anticipated future use of such material by the author must be stated at the time of submission. All existing copyright materials to be published must be cleared by the contributor(s) prior to submission.

Manuscripts must be accurate and preferably in the form of a diskette containing an electronic version in one of the common word processing formats. WORD is preferred but others are also acceptable. Whether or not an electronic version is submitted, two complete manuscript copies of the articles should be submitted. These should be preceded by a cover page stating the title of the article, the full name(s) of the author(s), identification data for each author (position and institution or other affiliation and complete mailing address). An abstract of about 150 words should be included. Manuscripts should be double-spaced, including references, single-side only on A4 size paper with a 2.5 cm margin on all sides, and be numbered serially. All references should be arranged in alphabetical and, for the same author, chronological order. In the text they should be placed in brackets as (Author'(s) name(s), date). In the reference list at the end the Author'(s) name(s) and initials followed by the date and title of the work. If the work is a book this should be followed by the publisherís name, place of publication and number of pages; or, if a journal article, by the title of the periodical, volume and page numbers.

Submission of electronic versions of illustrations is encouraged. Originals of any hardcopy illustrations submitted should be in black on tracing material or smooth white paper, with a line weight suitable for any intended reduction from the original submitted size. Monochrome photographs should be clear with good contrasts. Colour photographs are also accepted by prior arrangement with the Editorial Board. Originals of all illustrations should be numbered consecutively and should be clearly identified with the authorí(s) name(s) on the back. A complete list of captions printed on a separate sheet of paper.

All submitted material is accepted for publication subject to peer review. The principal author will be sent comments from reviewers for response, if necessary, prior to final acceptance of the paper for publication. After acceptance the principal author will, in due course, be sent proofs for checking prior to publication. Only corrections and minor amendments will be accepted at this stage. The Society is unable to provide authors with free offprints of items published in the Bulletin, but may be able to obtain quotations from the printer on behalf of authors who express, at the time of submission of proofs, a desire to purchase a specified number of offprints.

Enquiries and all correspondence should be addressed to the Editor-in-Chief, Hong Kong Meteorological Society Bulletin, c/o Hong Kong Observatory, 134A, Nathan Road, Kowloon, Hong Kong.